AN OPTIMUM DESIGN FOR A HYDROCLONE USING ELECTRICAL ANALOG TECHNIQUES

by

James Fred Beattie

Bachelor of Science

Oklahoma State University

Stillwater, Oklahoma

1959

Submitted to the Faculty of the Graduate School of
the Oklahoma State University
in partial fulfillment of the requirements
for the degree of
MASTER OF SCIENCE
August, 1961

AN OPTIMUM DESIGN FOR A HYDROCLONE USING

ELECTRICAL ANALOG TECHNIQUES

Thesis Approved:

J. A. Wiebelt

Thesis Adviser

W. H. Easton

Robert Thomson

Dean of the Graduate School

PREFACE

At the present time there is not an optimum design for a liquid-solid separation hydroclone. The need for a solution to this problem has prompted this investigation.

I sincerely wish to thank Dr. J. H. Boggs for the Teaching Assistantship. A generous thanks goes to Professor E. C. Fitch and Dr. John Wiebelt for their continued advice and encouragement throughout the course of this study as my advisers. I wish to thank Professor C. M. Leonard for proofreading my thesis. To my wife, Kathryn, goes my thanks for her patience and understanding.

TABLE OF CONTENTS

LIST OF FIGURES

LIST OF TABLES

CHAPTER I

INTRODUCTION

The hydroclone like the centrifuge, is essentially based on the principle of creating a centrifugal force field to effect the separation of solid particles, differing only in that the centrifuge produces the force by rotating the container as well as the fluid while the hydroclone container does not move. However, while the hydroclone does not have any moving parts, it does have a high specific mass transfer capacity, and is simple in construction and operation.

A brief description of the flow pattern and the reaction of the solids will acquaint the reader with the principles behind the hydroclone. The hydroclone consists of a cylindrical section mounted above a truncated cone. The fluid enters the hydroclone through a feed nozzle which is attached tangentially to the cylindrical section and at some predetermined angle (about 5 degrees) sufficient to give the inlet fluid a small downward component of velocity. Due to this small downward velocity component the fluid and solids in the hydroclone will not interfere with the entering feed. The hydroclone produces the centrifugal force necessary for separation by forcing the fluid to take a spiral path of decreasing radius. In the centrifugal force field developed, the particles at high velocities are thrown to the side of the hydroclone where they

settle down along the stationary side walls within the boundary layers due to gravity and are discharged through the underflow nozzle which is located at the apex of the truncated cone section, Fig. 1. The main flow pattern throughout the hydroclone separator consists of a double vortex, a large-diameter vortex spiraling downward along the hydroclone walls and leaving through the underflow nozzle; while the other, a smaller-diameter vortex spirals upward and leaves through the overflow nozzle or vortex-finder, Fig. 2. The flow leaving through the overflow nozzle is liquid from which the solid contaminants have been removed. The separation process depends on the centrifugal force which is proportional to the tangential velocity squared. However, the specific gravity of the medium largely controls the effective specific gravity of the separation. Also, it should be noted that the actual separation normally takes place at a somewhat higher specific gravity than that of the medium fed to the hydroclone. This is because the particles of the medium are restrained in the hydroclone longer than the fluid leaving through the vortex-finder, and the density of the medium in the separation zone within the hydroclone is, therefore, greater than that of the medium fed to the hydroclone through the feed nozzle. The equation

$$V_T = r\omega \tag{1-1}$$

gives the tangential velocity at any point within the fluid in the inner spiral, which is a forced vortex, while the equation

$$V = \frac{K_2}{r^n} \tag{1-2}$$

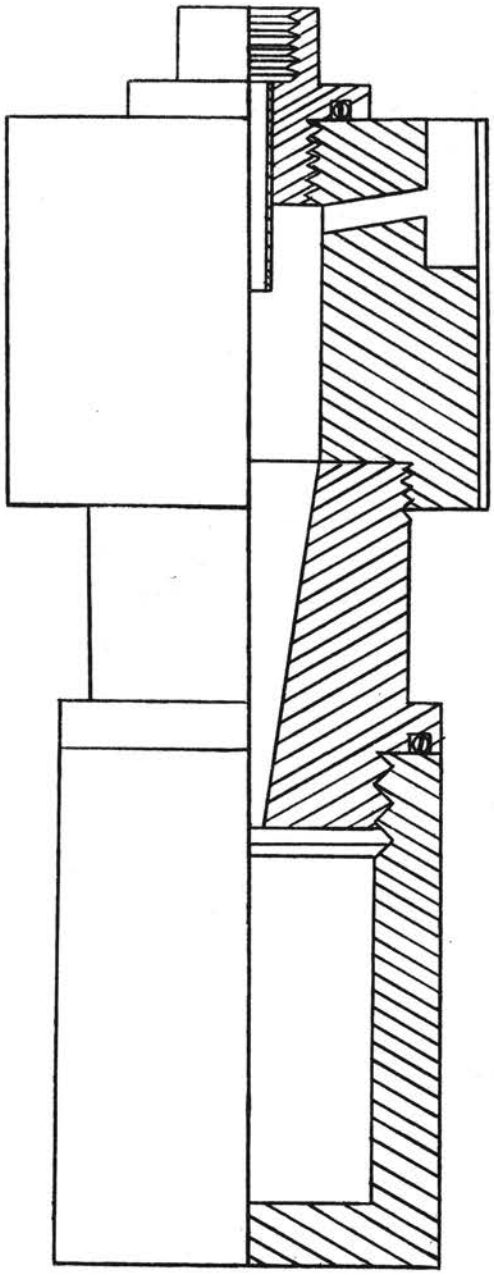

Figure 1. Hydroclone Cross Section

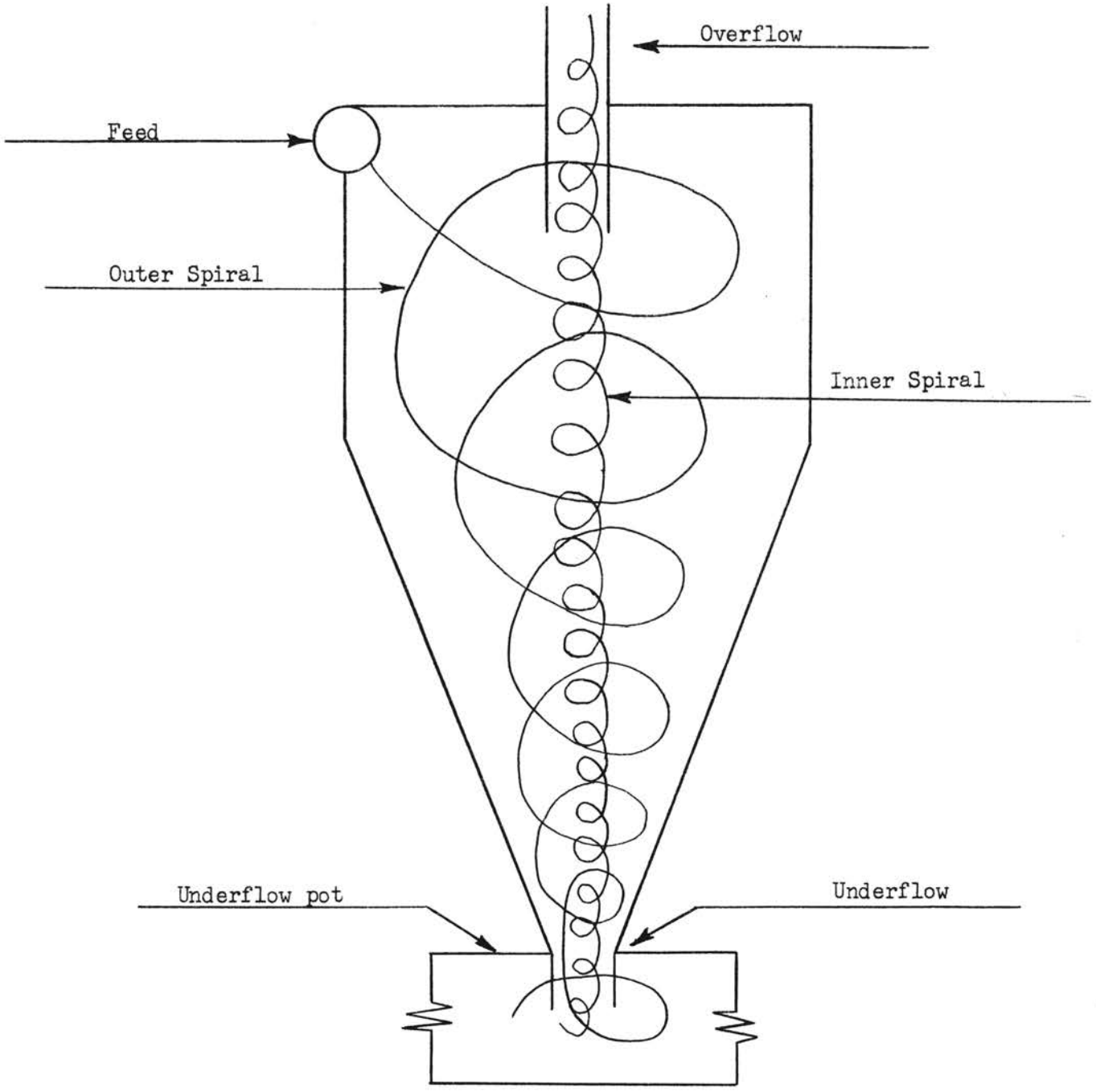

Figure 2. Flow Spirals in a Hydroclone

gives the velocity within the free-vortex or outer spiral. For a perfectly frictionless fluid moving in a circular path, the law of conservation of angular momentum requires the velocity to vary inversely as the radius or n is equal to one. Viscous forces within the fluid, however, will tend to prevent a velocity differential between adjacent layers of the rotation fluid. An extremely viscous fluid, might therefore, be expected to rotate with a nearly constant angular velocity.

The differential pressure at which the contaminated fluid is supplied also plays an important part in the liquid-solid separation hydroclone. An increase in velocity resulting from an increase in pressure differential causes higher centrifugal forces within the hydroclone which will result in a decrease in particle size which will be discharged at the overflow. However, this effect is limited due to the decrease in the time that the contaminated fluid is within the hydroclone. If the pressure losses are large or the initial supply pressure is low, the centrifugal force in the inner spiral or vortex will not be large enough to completely remove all of the contaminating particles causing the fluid leaving through the overflow nozzle or vortex-finder to be contaminated. However, one disadvantage of having a high inlet pressure is that it tends to reduce the operating life of the hydroclone.

The inlet centrifugal force can be calculated easily by dividing the volume rate of flow by the feed nozzle cross sectional area to obtain the inlet tangential velocity. Squaring this term and dividing

by the cylindrical radius of the hydroclone gives the centrifugal force.

The underflow nozzle is the most critical of the operating variables. If this opening is too large, the underflow will contain a considerable amount of liquid. However, if the nozzle is too small, it may prevent the discharge of the large particles as fast as they reach the underflow outlet, thus causing some of the larger and coarser particles to be forced out through the vortex-finder or overflow nozzle contaminating the fluid at exit.

The general design features of a hydroclone will be predetermined in this investigation. It is accepted that, in general, the vortex-finder or overflow nozzle should extend to a point just below the bottom of the feed inlet to the hydroclone to keep the incoming fluid from passing directly out through the vortex-finder without entering the centrifugal force field. Also, the distance between the top of the inlet nozzle and the bottom of the cylindrical section should be kept at a minimum to minimize turbulence which results in an increase in pressure loss and an overall decrease in efficiency.

CHAPTER II

PREVIOUS INVESTIGATIONS OF HYDROCLONES

The liquid-solid hydroclone is similar in construction and operation to the older and more familiar gas cyclone dust collector. However, only in recent years has real progress been made in developing and understanding the phenomenon which occurs within the hydraculic cyclone, or more commonly called, hydroclone.

Two empirical equations of importance were developed by Dahlstrom (3) for pressure drop and solid elimination efficiency. The first equation is for the prediction of pressure drop through a hydroclone in terms of flow rate. It is stated as follows:

$$\frac{Q}{\sqrt{\Delta P}} = K(D_{of}\ D_i)^{0.9} \qquad (2\text{-}1)$$

The constant K was found to be dependent on the included cone angle (θ), the distance between the conical section and the overflow nozzle (h), and the type of the underflow discharge, Fig. 3.

The second empirical expression involves solid elimination efficiency. This equation was developed to determine the 50%-point. The 50%-point represents the particle which reports 50% by weight to the overflow nozzle and 50% by weight to the underflow nozzle. The 50%-point also provides a limit of extraction efficiency because

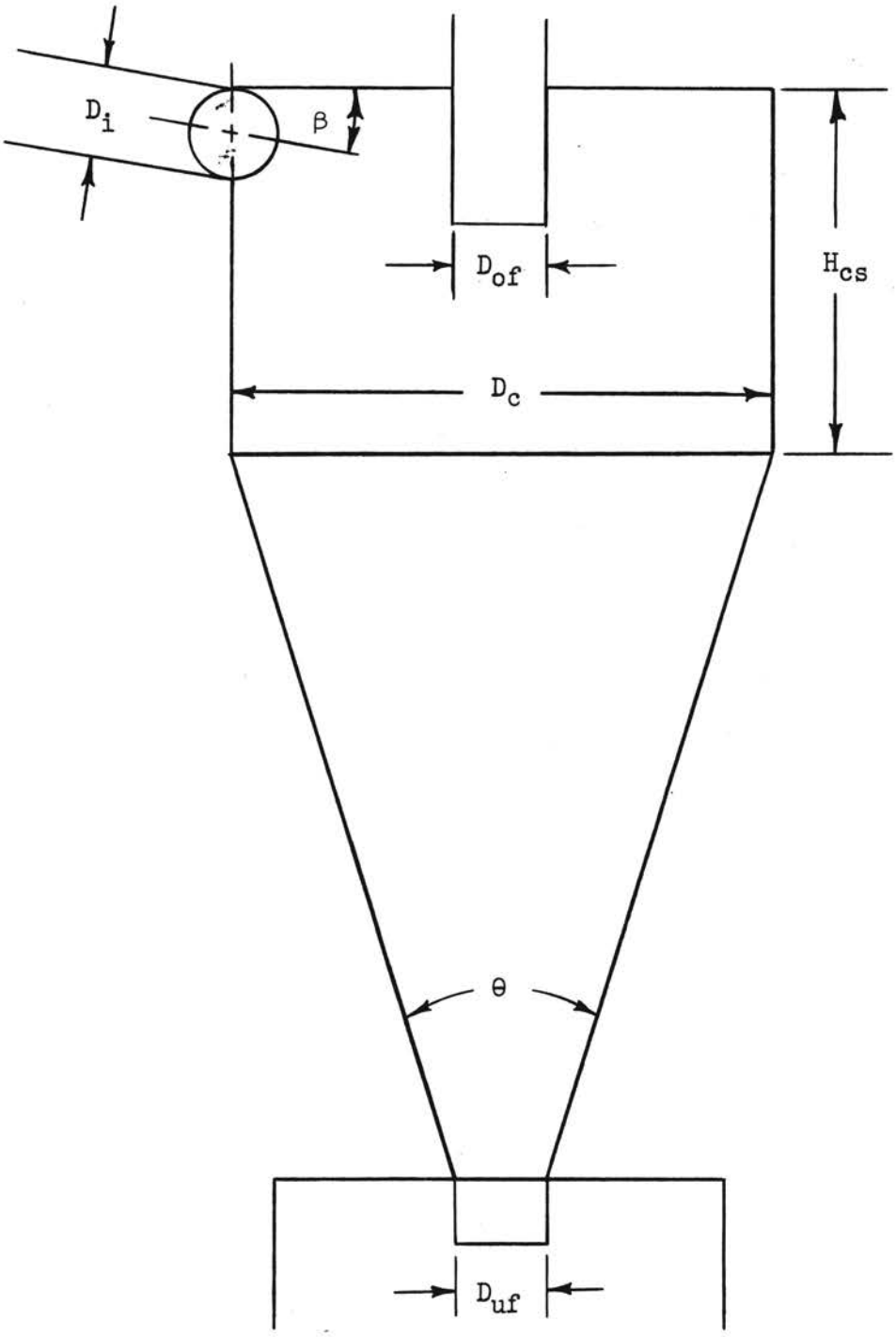

Figure 3. Hydroclone Dimensions

very little material of similar specific gravity but larger in size, will be found in the stream leaving the overflow nozzle. Also, only a relatively small amount of particles finer than the 50% point will be found in the stream leaving the underflow nozzle.

Dahlstrom's (1) second empirical equation is expressed as follows:

$$D_{50} = \frac{K(D_{of}\ D_i)^{\frac{1}{1.189}}}{Q} \left[\frac{2.73-1.00}{\rho_s - \rho_L}\right]^{\frac{1}{2}} \qquad (2\text{-}2)$$

Driessen (2) and Criner (3) proposed the concept of the equilibrium radius. Since any particle within a hydroclone is undergoing an acceleration in the radial direction due to centrifugal force, it must eventually reach a position at which the resultant radial settling force of the particle predicted by Stokes' Law will equal the inward radial drag force due to the circulating fluid. This point for a given particle diameter is defined as the equilibrium radius. Also, an equilibrium envelope may be established with the condition that the inner radius of the forced vortex must first be located. Therefore, all particles of a given specific gravity in equilibrium with the maximum centrifugal force generated and the radial drag force would exit in equal amounts with the streams leaving through the overflow and underflow nozzle.

By using a generalized correlation developed by Yosheoka and Hotta (1) we have

$$\Delta P = \frac{KQ^2}{D_{ci}^{0.9}\ D_i^{1.2}\ D_{of}^{1.9}} \qquad (2\text{-}3)$$

in which K is a function of the fluid system and the hydroclone inside surface finish. This equation is for miniature hydroclones which have overflow and underflow diameters between 0.167 D_c to 0.333 D_c and a hydroclone length between 5 D_c to 8 D_c.

Nurni, Haas, Whatley, and Engel (4) made studies for dimensioning a series of hydroclones to separate particles of one to ten microns in size. From Eq. (2-3), a plot of log ΔP versus log Q should give a straight line with a slope of two. However, a plot of the experimental results of more than thirty hydroclones with an inside diameter of 0.16, 0.25, and 0.40 inches (midget hydroclones) showed that the slope varies from 2.10 to 2.45 with an average value of 2.27. Therefore, by rewriting the generalized correlation to reflect a slope of 2.27, the following equation was developed: (4).

$$\Delta P = \frac{K' Q^{2.27}}{D_{ci}^{0.8} D_i^{1.3} D_{of}^{2.0}}$$

This equation has a smaller variation in K', with the maximum occurring when a small centrifugal field is developed within a hydroclone which has a poorly finished inside surface.

By introducing smoke and dust particles into the feed of a 12-inch diameter gas cyclone, C. B. Shepherd and C. E. Lapple (5) studied the flow patterns within the centrifugal fields of a cyclone, verifying the existence of a double vortex flow pattern. Also, by measuring the angle made by rayon streamers with the horizontal, they have shown that the outer vortex descends at a rate just

sufficient to prevent interference on successive revolutions of the incoming feed. This rate of descent was equal to approximately the height per revolution of the inlet feed duct with the variation being due to the inlet feed expanding both vertically and horizontally upon entering the gas cyclone. This expansion is a function of the cyclone's nozzle proportions and the inlet pressure.

Kelsall (6) found experimentally that the main flow pattern of a liquid-solid hydroclone is concentrated in the outer free vortex caused by the feed entering tangentially. Within this free vortex is a narrow, almost cylindrical, central fluid tube. This central tube consists of a forced vortex that is fed from the free vortex after it has exited through the underflow nozzle and it has the same direction of rotation with respect to the hydroclone's axis, but leaves through the overflow nozzle. Kelsall also proved experimentally that critical separation occurs at the outer radius of the forced vortex or the inner radius of the free vortex. This radius has been found to be approximately equal to the hydroclone's overflow nozzle when it is relatively small. Kelsall used the following relation for the tangential velocity in a free vortex:

$$V_T = \frac{K}{r^n} \qquad (1\text{-}2)$$

in which the exponent n varied from a positive one for a frictionless fluid when the law of conservation of angular momentum applies, to a negative one for a solid where constant angular velocity applies. This equation of tangential velocity predicts an infinite velocity

at the hydroclone's axis. Kelsall showed experimentally that the free vortex flow appears to go through a sharp transition to form a forced vortex in the region of a radius approximately equal to the overflow or vortex-finder radius where the tangential velocity distribution in the forced vortex is as follows:

$$V_T = K'r \tag{2-5}$$

Banesji and Roy (7) predicted that the exponent in Eq. (1-2) would be 0.50, based upon the Navier-Stokes' equation, after making certain simplifying assumptions about the free vortex boundary conditions and assuming viscous flow.

The pressure drop in a hydroclone from Bernoulli's theorem is:

$$\Delta H = H_i - H_E = \frac{V_i^2 - V_e^2}{2g} \neq F \tag{2-6}$$

in which $H_i - H_E$ is the change in velocity head between the inlet to the hydroclone and the overflow discharge nozzle and F is the loss of mechanical energy due to friction. This equation holds true if the relatively small amount of fluid and contaminants issuing from the underflow nozzle is neglected. Rewriting H and F in terms of the initial velocity head, Eq. (2-6) can be written for incompressible flow in the following form:

$$\frac{2g\Delta H}{V_i^2} = H_v = F_v - 1 \neq \left[\frac{A_i}{A_E}\right]^2 \tag{2-7}$$

or

$$H_v = F_{ev} \neq F_{cv} - 1 \neq \left[\frac{A_i}{A_E}\right]^2$$

The pressure drop in the vortex-finder or overflow nozzle can be calculated by using Fanning's equation which gives:

$$F_{ev} = \frac{4JL_E}{D_E} \left[\frac{A_i}{A_E}\right]^2 \qquad (2\text{-}8)$$

where the coefficient of friction J is assumed to be 0.0055. (5). Since this coefficient of friction is quite small, the friction loss in the exit or overflow nozzle becomes insignificant. Any additional friction or recovery effects due to the presence of swirling flow will be included with F_{cv}. However, according to Shepherd (5), this item is small, so it will be neglected in this investigation; therefore, the friction loss in the hydroclone in terms of the number of inlet velocity heads is:

$$F_{cv} = \frac{D_4}{D_5\ D_6\ (0.5)} \qquad (2\text{-}9)$$

where D_4 is the diameter at which the tangential velocity of the free vortex equals the inlet velocity; D_5 is the diameter at the inner edge of the free vortex; and D_6 is the inner diameter of the forced vortex. According to C. E. Lapple and C. B. Shepherd the fluid stream entering the hydroclone may expand laterally if the inlet width is less than the annular width. This lateral expansion will be proportional to b/c. Applying the hydrodynamic formula for a sharp expansion loss yields:

$$F_o = \frac{(V_o - V)^2}{2g} = \frac{V_o^2}{2g} \left[1-K_1\left(\frac{b}{c}\right)\right]^2 \qquad (2\text{-}10)$$

Two methods of designating the classification point or separation power of the hydroclone are available in the literature. The first

method predicts the size of the particles which would report 50% by weight to the overflow and the underflow nozzle. The second method represents the particle diameter in microns at which 1.5% by weight of the underflow contaminants would be coarser than that found in the overflow fluid. This method is called the mesh of separation. The most common method of measuring solid elimination efficiency is the determination of the 50% point.

Dahlstrom (1) found that the solid elimination efficiency is a function of the solid specific gravity. Also, since the specific gravity of the particles will have such a wide range of values, a continuous curve of the 50% point versus particle specific gravity count be developed from Eq. (2-2).

Kelsall (8) studied the hydraulic cyclone to determine the effect of changing the length of the vortex-finder on the solid-elimination efficiency. In this study, tests were carried out with the length of the vortex-finder varying from 5/8 inch to 4 inches, measured from the top of the hydroclone. The conditions were as follows:

1st run: Pressure-6.0 psi; D_i-3/8 inch; D_o-1/4 inch; D_u-1/8 inch.
2nd run: Pressure-15 psi; D_i-1/4 inch; D_o-1/4 inch; D_u-1/8 inch.
3rd run: Pressure-15 psi; D_i-3/8 inch; D_o-1/4 inch; D_u-1/8 inch.

The results of these tests show that solid elimination efficiency increased for the smaller size particles as the length of the vortex-finder is decreased and the elimination efficiency of the larger

particles decreases noticeably as the vortex-finder decreases in length. The second run indicated that for some particles the solid elimination efficiency increased to a maximum and then decreased with further reduction in the length of the vortex-finder.

Kelsall's explanation for the results is that the majority of the particles in the small-size ranges when discharged through the overflow nozzle (vortex-finder) has passed down through the hydroclone outside the zero-vertical-velocity envelope. Therefore, after reaching the lower region of the hydroclone, the particles have been carried inward by the radial velocity components and upward by the high velocity upward flow near the center. As the radial velocity tends to decrease as the bottom of the vortex-finder is approached and the centrifugal acceleration remains unchanged, the particles tend to move outward.

If the assumption that all of the larger particles that are discharged through the overflow nozzle originate from turbulent flow is correct, an increase in the vortex-finder length would cause a longer time interval for these particles to be eliminated from the turbulent flow. Also, if the same or similar velocity profiles are sustained within the turbulent flow for the entire length of the vortex-finder, a higher solid elimination efficiency through the vortex-finder or overflow nozzle would be effected, because particles leaving the turbulent flow section would be redistributed within the feed section and a majority would enter the main downward flows within the hydroclone and leave through the underflow nozzle.

With a short vortex-finder many of the larger particles would leave the area of turbulent flow and pass out through the overflow nozzle. Also, the time available for low density particles to leave the vertical flow patterns and reach the vortex-finder directly is much greater than when a long vortex-finder is used. Therefore, a greater fraction of the particles will be recirculated in the feed section of the hydroclone, where mixing occurs, and may make repeated passes through the main centrifugal flow pattern. Thus the shorter vortex-finder would lead to higher solid elimination efficiencies for smaller size particles. This result would be expected and has been experimentally-proven.

Haas (9) is the only author to suggest the use of an underflow pot in determining the optimum dimension ratios. An underflow pot is a closed reservoir connected to the underflow nozzle to trap and hold contaminants which have gravitated along the stationary side walls of the hydroclone within the quiescent boundary layers. Due to the pot being a closed reservoir an equal amount of solution must return through the underflow nozzle and back into the mixing region. The time delay between mixing will permit some of the particles to settle out in the underflow pot. This will result in a greater solid elimination efficiency. However, contaminants collected by a hydroclone might not settle out due to either the presence of thermal convection currents, turbulence, or their small size. The ratio of the volume flow rates of the induced underflow to the hydroclone-inlet fluid is determined by the geometry of the

hydroclone. Ratios of zero to four percent were possible without large changes in hydroclone efficiency.

When contaminants first enter the hydroclone their behavior is governed by the acceleration force which is a function of the centrifugal field within the hydroclone and the fluid viscosity. Equating forces in the horizontal plane yields:

$$F_a = F_c - F_d \tag{2-11}$$

This equation represents the movement of a particle subjected to a centrifugal field within a viscous medium.

Driessen (2) plotted the Navier-Stokes' equations on polar coordinates and assumed coaxial cylinders existed about the origin. Since coaxial cylinders can be produced from a hydroclone by passing two imaginary planes normal to the hydroclone axis a correlation was obtained. This was done by assuming that the flow rate on either side of the normal planes were equal and that the velocity component in the plane parallel to a given axis were zero. Applying initial conditions and replacing the partial derivatives with ordinary derivatives, the Navier-Stokes' equation becomes:

$$-\frac{A}{2\pi r^2}\frac{d(V_R)}{dr} = \upsilon \frac{d}{dr}\left[\frac{1}{r}\frac{d(V_R)}{dr}\right] \tag{2-12}$$

in which $A = -V_R\, r2\pi$ and changing υ, the kinematic viscosity to β, the coefficient of turbulent viscosity.

Since the radial velocity is a function of the radius of the coaxial cylinder, Eq. (2-12) may be reduced to the following equation:

$$\frac{df(r)}{f(r)} = \left[- \frac{A}{2\pi\beta} \neq 1 \right] \frac{dr}{r} \tag{2-13}$$

From Eq. (2-13)

$$- \frac{A}{2\pi\beta} \neq 1$$

is arbitrarily set equal to n. For a special case of n equal to a negative one, the coefficient of turbulent viscosity β, will equal $A/4\pi$. By substituting n into Eq. (2-12) and integrating, the following equation is obtained:

$$V = \left[\frac{C}{n \neq 1} \right] r^n \neq \frac{C_1}{r} \tag{2-14}$$

For a special case of $n = 1$ or $\beta = A/4\pi$, Driessen (2) found Eq. (2-14) to be within close agreement with the experimental value of n. Upon evaluation of the constants C and C_1 using a given set of boundary conditions and letting $n = 1$, Driessen developed an equation for the tangential velocity of a two-dimensional vortex in a viscous fluid that is referred to as the "Logarithmic Solution." This equation is as follows:

$$V = \frac{V_2 r_2}{r} \frac{1 \neq \ln \frac{r}{r_1}}{1 \neq \ln \frac{r_2}{r}} \tag{2-15}$$

In Driessen's (2) and Criner's (3) in Eq. (2-12) and Eq. (2-15), several assumptions were made. These are listed as follows:

(a) The flow is steady, which means that the components of velocity and pressure are the same at a time t, and at a time $t + dt$. Therefore,

$$\frac{du}{rd\theta} = \frac{dv}{dt} = \frac{dp}{dt} = 0.$$

(b) By applying axial symmetry to the axis of the vortex, all pressure and velocity components are equal along the coaxial cylinders. Therefore, there is no change in these vectors if the θ coordinate is changed alone. Therefore

$$\frac{du}{rd\theta} = \frac{dv}{rd\theta} = \frac{dw}{rd\theta} = \frac{dp}{rd\theta} = 0.$$

(c) As was previously stated, two-dimensional flow was assumed; thus, the velocity in the Z-direction will be equal to zero as well as all of the derivatives. Therefore, the change in the components (u, v, p) with respect to z will be zero.

$$\frac{du}{dz} = \frac{dv}{dz} = \frac{dp}{dz} = 0.$$

Furthermore, it was assumed that the differences in pressure within the hydroclone's system were such that the fluid could be considered to be incompressible, so that the mass density (ρ_L) would be constant and the change of pressure with respect to any variable would be equal to zero.

Matschke developed and tested the following design criteria for a large hydroclone (3 to 36 inches in diameter) and found the test

results to be satisfactory. A brief outline of the geometric guides applied by Matschke is as follows:

1. The included angle (θ), should be as small as possible and still provide the necessary internal flow pattern.

2. The bottom of the vortex-finder should be six inches or one hydrocclone diameter, whichever is less, below the transition point between the conical and cylindrical sections.

3. To allow the entering fluid to descend at least one inlet nozzle diameter in the first revolution, the inlet-feed nozzle should slope downward to make a small angle (about 5^{o}) with the top of the hydroclone.

4. From the following ratios the inlet nozzle and overflow nozzle dimensions with respect to the hydroclone diameter are determined:

$$\frac{2d_i \neq d_o}{d_c} = 0.35 \text{ to } 0.70 \qquad (2\text{-}16)$$

$$\frac{d_o}{d_1} = 1.0 \text{ to } 1.6 \qquad (2\text{-}17)$$

5. To minimize secondary flow (turbulence) which results in an overall decrease in solid elimination efficiencies, the distance between the top of the inlet-feed nozzle and the hydroclone top should be kept at a minimum.

In recent discussions and experimental tests made by Moder (13), a more general recommendation as to hydroclone designs was established as follows:

1. The included angle (θ) should be maintained as small as possible, consistent with head room available. It should range between 15 to 20°.

2. The overall height of the hydroclone should be at least six inches and, in general, two hydroclone diameters are sufficient.

3. The inlet-feed nozzle should be such that the inlet-feed descends a distance corresponding to at least one inlet nozzle diameter per revolution at the hydroclone wall.

4. The distance between the top of the hydroclone and the top of the inlet-feed nozzle should be kept at t minimum to maintain solid elimination efficiencies high by decreasing turbulent flow due to the expanding inlet feed.

5. The overflow nozzle must be even with the center of the inlet-feed nozzle for volume splits of about 50%. For volume splits less than 50%, the sink solids separation could be improved slightly by extending the overflow nozzle about one-half of the hydroclone diameter below the inlet-feed nozzle.

6. The product of the inlet-feed nozzle diameter and the overflow nozzle diameter ($d_i d_o$) is fixed by the required flow and specified pressure drop as indicated by the following equations:

$$Qd_i = 0.37(H_i)^{0.44} (d_c)^{1.8} \tag{2-18}$$

$$\frac{2d_i \neq d_o}{d_c} = 0.35 \text{ to } 0.70 \tag{2-19}$$

and

$$\frac{d_o}{d_i} = 1.0 \text{ to } 1.6 \tag{2-20}$$

7. In general, the hydroclone diameter can be calculated from the following relation:

$$D_c = 2(2d_i \not{} d_o) \tag{2-21}$$

The extensive literature on the hydroclone contains little information about the design functions for an optimum design to satisfy a given set of initial conditions. If a thorough report was available on the variables included in the design of a hydroclone, their uses would be greatly increased and the design established analytically.

CHAPTER III

STATEMENT OF PROBLEM

The mathematical expression that has been developed and used for predicting liquid-solid separation within hydroclones has not included the effects of turbulent viscosity or the force required to accelerate the mass of the fluid set in motion by the acceleration of the particle (pressure drag). According to Kelsall's (8) more recent work in hydroclone behavior, the importance of turbulent mixing and turbulent viscosity in the feed section and along the outside walls of the vortex-finder may be of prime importance due to shock effects resulting from expansion of the fluid.

The purpose of this investigation was to develop a mathematical expression including the effects of turbulent viscosity and pressure drag. This expression was then to be evaluated to give an accurate assessment of the effect of the several hydroclone variables on liquid-solid separation by use of a Donner electrical analog. The results were to be analyzed for the purpose of developing an optimum design.

CHAPTER IV

ANALYTICAL DEVELOPMENT

To predict the solid elimination ability of a hydroclone, it is necessary to know whether a particle has sufficient time to move from a position near the axis of the hydroclone to a position of greater radius than the radius of the vortex-finder within the hydroclones. Thus, the particle will be forced to the walls and exit through the underflow nozzle.

This investigation provides an equation which can be solved for a given time in terms of the hydroclone's radius and the distance a given-size particle if from the hydroclone's axis. In this analysis, the following basic assumptions were made:

1. The flow pattern predicted by Criner (10) accurately describes the flow pattern of the fluid within a hydroclone.

2. Solids moving through the hydroclone assume the velocity of the fluid at every point except where motion relative to the fluid is caused by centrifugal forces.

3. The air core in the overflow nozzle will be eliminated by correct application of back pressure to the underflow nozzle.

4. The radial acceleration of a particle in a hydroclone is large enough to be considered.

5. Gravity and buoyant forces of a particle are small enough to be neglected.

Figure 4 shows a velocity field existing within the hydroclone boundary. The fluid enters tangentially at the outer boundary of the cylindrical portion, thus causing a two-dimensional vortex type flow to exist at every axial cross section.

In order to obtain the equations of motion for viscous fluids, the relationships between the stresses and velocity gradients must be established. However, since Navier-Stokes' equations are based on this relationship, they shall be used without any discussion as to their development.

When the particle first enters the hydroclone its behavior is governed by the acceleration force which is a function of the centrifugal field and the fluid viscosity. Referring to Fig. 5 and summing forces in the horizontal plane yields:

$$F_a = F_c - F_d \tag{4-1}$$

which is Stokes' Law for viscous flow (1). These forces represent the motion of particles subjected to a centrifugal field within a viscous medium. Equating forces gives:

$$\frac{4}{3}\pi\left[\frac{D_o}{2}\right]^3 \rho_s \frac{dV_R}{dt} = \frac{4}{3}\pi\left[\frac{D_o}{2}\right]^3 \left[\rho_s - \rho_L\right]\frac{V_T^2}{r} \tag{4-2}$$

$$-6\pi\frac{D_o}{2}\bar{\mu}_o\ V_R - C_D\frac{\rho_L}{2}V_R^2\pi\left[\frac{D_o}{2}\right]^2$$

in which $\bar{\mu}_o$ is turbulent viscosity. Simplifying, results in

Plane Perpendicular to

Hydroclone Axis

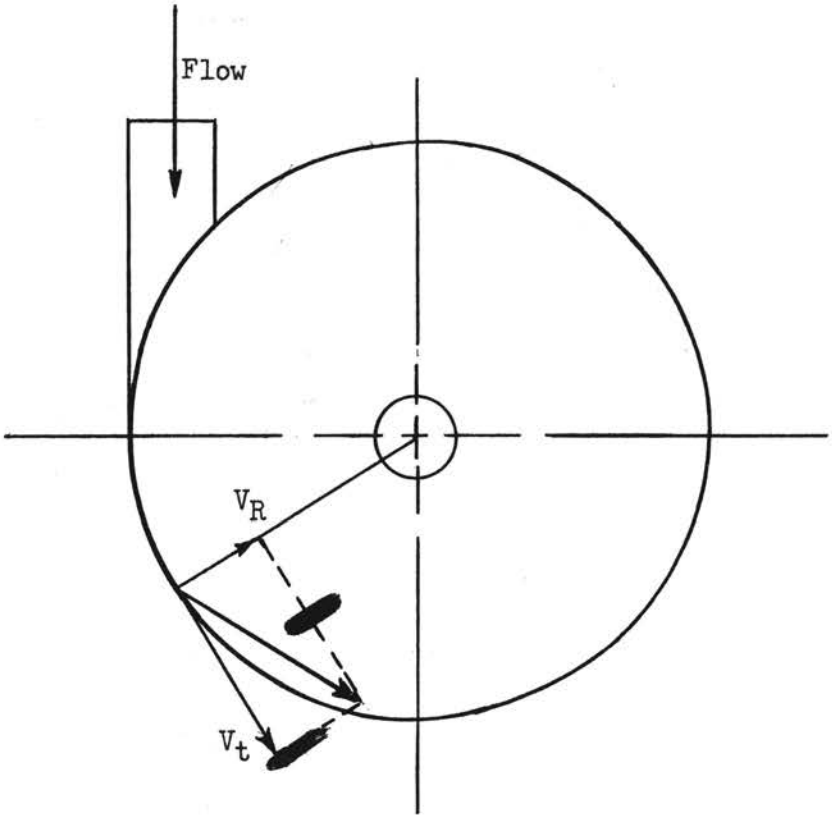

Figure 4. Velocity Field in a Hydroclone

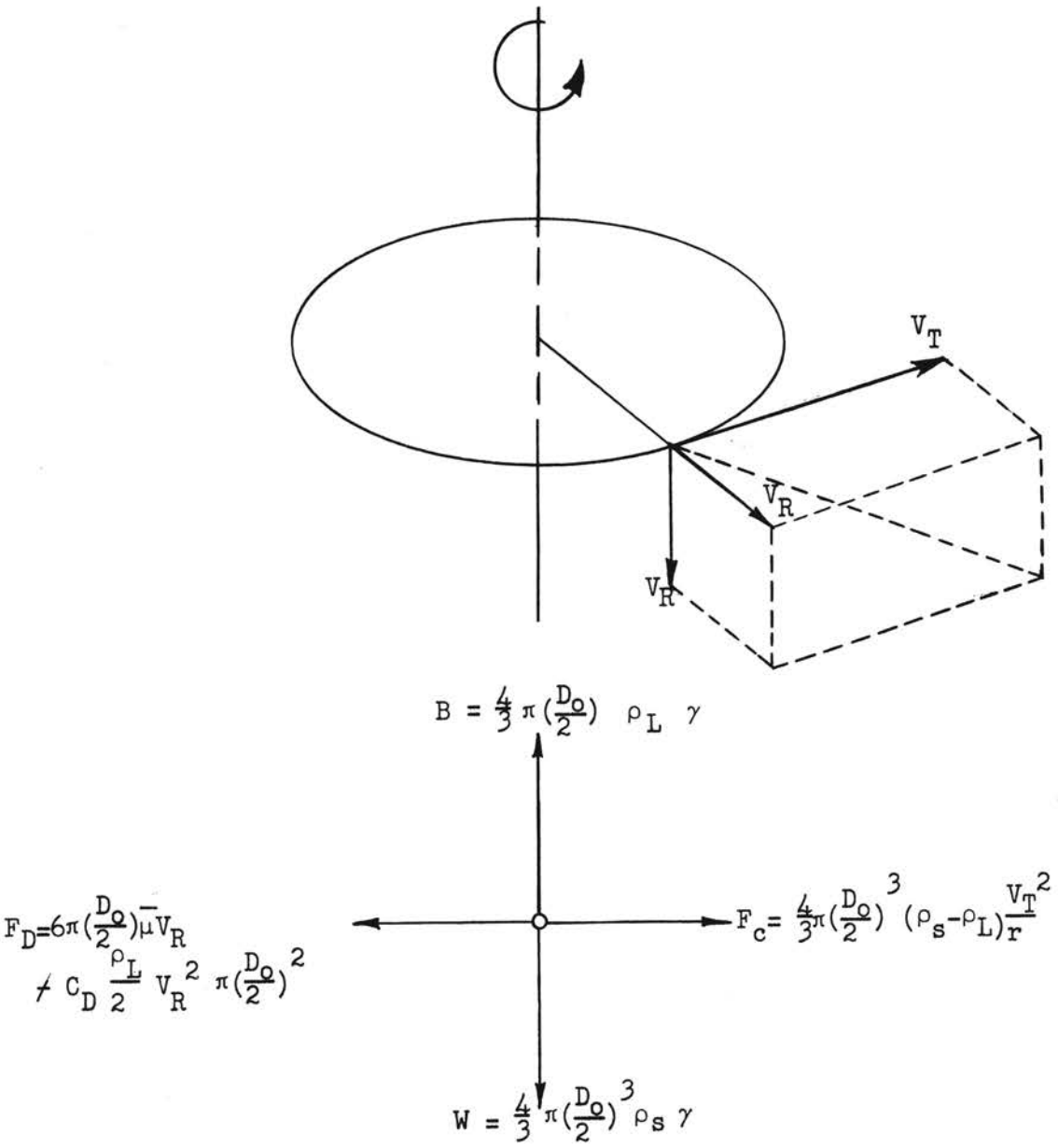

Figure 5. Forces Acting on a Particle in a Hydroclone

$$\frac{dV_R}{dt} = \frac{[\rho_s - \rho_L]}{\rho_s} \frac{V_T^2}{r} - \frac{C_D}{\frac{4}{3}} \left[\frac{V_R}{\frac{D_o}{2}}\right]^2 \frac{\rho_L}{2\rho_s} - \frac{18}{D_o^2} \frac{\bar{\mu}_o}{\rho_s} V_R \qquad (4\text{-}3)$$

where ρ_L is assumed to remain relatively constant to a small degree, varying only with temperature.

Tietjens (11) found that to accelerate a sphere in an ideal fluid it is not only necessary to exert a force equal to the product of the mass of the sphere and its acceleration, but an additional force is required to accelerate the mass of the fluid particles set in motion by it. This additional force is equal to the product of the acceleration of the sphere and mass of an amount of fluid equal to half its volume. Hence, Eq. (4-2) becomes,

$$\frac{dV_R}{dt} = \left[\frac{\rho_s - \rho_L}{\rho_s + \frac{\rho_L}{2}}\right] \frac{V_T^2}{r} - \frac{C_D}{\frac{4}{3}} \frac{V_R}{\frac{D_o}{2}} \left[\frac{\rho_L}{2\rho_s + \frac{\rho_L}{2}}\right] - \frac{18}{D_o^2} \frac{\bar{\mu}_o V_R}{\rho_s + \frac{\rho_L}{2}} \qquad (4\text{-}4)$$

Writing V_T in terms of the tangential velocity at the inlet, $r=r_c$, it is found that

$$V_T^2 = \frac{V_{oi}^2 r^{2n}}{r_c^{2n}} \qquad (4\text{-}5)$$

in which $n = -0.5$. Therefore, Eq. (4-3) becomes

$$\frac{dV_R}{dt} = \left[\frac{\rho_s - \rho_L}{\rho_s + \frac{\rho_L}{2}}\right] \frac{V_{oi}^2 r^{2n-1}}{r_c^{2n}} - \frac{C_D}{\frac{4}{3}} \left[\frac{V_R}{\frac{D_o}{2}}\right] \frac{\rho_L}{\frac{r\rho_s + \rho_L}{2}} - \frac{18}{D_o^2} \frac{\mu_o V_R}{s + \frac{\rho_L}{2}} \qquad (4\text{-}6)$$

According to Tietjens (11), a change in the Reynolds number causes a change in the drag coefficient. Hence,

$$D = f(N_R) \frac{Q\rho V^2}{2} \tag{4-7}$$

From a plot of N_R versus C_D, Tietjens (11) established that

$$C_D = \frac{32}{N_R} \tag{4-8}$$

in which

$$N_R = \frac{V\ D}{\bar{\mu}} \tag{4-9}$$

Substituting Eq. (4-9) into Eq. (4-7) gives:

$$DRAG = \frac{32}{8} \pi \bar{\mu} D\ V_R \tag{4-10}$$

Therefore, the expression (4-6) may be rewritten as:

$$\frac{d^2r}{dt^2} = \frac{\rho_s - \rho_L}{\rho_s + \frac{\rho_L}{2}} \left[\frac{V_{oi}}{r_c^n}\right]^2 r^{2n-1} - \frac{24\ \bar{\mu}_o\ V_R}{D_o^2 \left[\rho_s + \frac{\rho_L}{2}\right]} \tag{4-11}$$

Electrical analog techniques will be applied to Eq. (4-11) in the next chapter to simplify its practical application. First, a relation for known flow patterns in a typical hydroclone is needed. The following analytical development is for the tangential velocity in terms of known quantities with no new variables.

Under certain conditions, the flow around a vortex can be calculated if the system is considered as two-dimensional. This can be done by passing two imaginary planes through the hydroclone normal to its axis and assuming that the flow under or over these planes would be identical to that bounded by the imaginary planes so that all flow parallel to the given axis will be zero.

The Navier-Stokes' equations which govern viscous flow will be converted to cylindrical polar coordinates. As was previously stated two-dimensional flow was assumed; therefore, the velocity in the Z-direction will be zero as well as all its derivatives. Therefore, the change in the components (u, v, p) with respect to z will be equal to zero. Also, since the flow is polar symmetrical, which means that the velocity and pressure remain constant on coaxial circles, the Navier-Stokes' equations simplify to:

$$\frac{\partial V_R}{\partial t} + \frac{V_R \partial V_R}{\partial r} - \frac{V^2}{r} = \frac{\mu}{\rho} \left(\nabla^2 V_R - \frac{V_R}{r^2}\right) \tag{4-12}$$

$$\frac{\partial V}{\partial r} + \frac{V_R \partial V}{\partial r} + \frac{V_R V}{\partial r} = \frac{\mu}{\rho} \left(\nabla^2 V_R - \frac{V}{r2}\right) \tag{4-13}$$

$$\nabla^2 = \frac{\partial^2}{\partial r^2} + \frac{1}{r} \frac{\partial}{\partial r} \tag{4-14}$$

in which

$$\frac{\partial P}{\partial r} = \frac{\partial r}{r \partial \theta} = 0$$

and the external body forces per unit mass are equal to zero.

For the case of polar symmetrical steady flow, Eq. (4-9) and Eq. (4-10) can be simplified by applying limiting conditions. Only Eq. (4-9) and Eq. (4-11) will be used in this analysis and the limiting conditions will be listed as follows:

(a) The flow is steady, which means that the velocity and pressure are the same at a time t and a time t + dt. Therefore,

$$\frac{\partial V_R}{\partial t} = 0 \qquad \frac{\partial V}{\partial t} = 0$$

(b) The difference in pressure, $\triangle P$, within the system is small enough that the fluid medium may be considered as incompressible so that the mass density (ρ_L) will be constant and the change in pressure with respect to any variable will be equal to zero. By assuming the fluid medium to be incompressible, the conditions of continuity

$$\frac{\partial(V_R r)}{\partial r} = \frac{\partial(Vr)}{\partial r} = 0$$

show that the amount of fluid flowing perpendicular through the imaginary plane normal to the hydroclone's axis is constant.

Applying these final conditions and replacing the partial derivatives with ordinary derivatives, Eq. (4-9) and (4-11) simplified become

$$V_R \frac{dV}{dr} + \frac{V_R V}{r} = \frac{\mu}{\rho}\left(\nabla^2 V - \frac{V}{r^2}\right) \tag{4-15}$$

in which

$$\nabla^2 = \frac{d^2}{dr^2} + \frac{1}{r}\frac{d}{dr} \tag{4-16}$$

Substituting Eq. (4-13) into Eq. (4-12) gives

$$V_R \frac{dV}{dr} + \frac{V_R V}{r} = \frac{\mu}{\rho}\left(\frac{d^2V}{dr^2} + \frac{1}{r}\frac{dV}{dr} - \frac{V}{r^2}\right) \tag{4-17}$$

Reducing Eq. (4-14) gives

$$\frac{V_R}{r}\left[\frac{d(Vr)}{dr}\right] = \frac{\mu}{\rho}\frac{d}{dr}\left[\frac{1}{r}\frac{d(Vr)}{dr}\right] \tag{4-18}$$

Now solving Eq. (4-18) for the radial velocity V_R and substituting it into Eq. (4-11) yields the final form ready for application to a specific hydroclone as follows:

$$\frac{d^2r}{dt^2} = \frac{\rho_s - \rho_L}{\rho_s + \frac{\rho_L}{2}} \left[\frac{V_{oi}}{r_{ci}^n}\right]^2 \frac{1}{r^2} - \left[\frac{24\bar{\mu}_o}{D_o^2}\right] \frac{1}{\rho_s + \frac{\rho_L}{2}} \frac{dr}{dt} \qquad (4\text{-}19)$$

CHAPTER V

APPLICATION OF ELECTRICAL ANALOG

Before solving Eq. (4-19) on the Donner electrical analog, all of the constants were determined from fixed initial conditions. These limiting conditions are listed as follows:

Q_o = 8 gpm = 308 $in.^3/sec$

V_{oi} = 2500 in./sec

r_i = 1/16 in.

r_o = 1/8 in. (Partial displacement from axis)

r_{ci} = 1/4 in.

D_o = 100 micron = 3.94×10^{-3} in.

ρ_L = 1.65 $lb\text{-}sec^2/ft^4$

ρ_s = 4.85 $lb\text{-}sec^2/ft^4$

$\bar{\mu}_o$ = 4.2×10^{-4} $lb\text{-}sec/ft^2$

$D_{uf} = D_{of} = D_i = D_{ci}/4$

Having solved for the constants, the selection of time and magnitude scales is made. This was done by letting one inch equal 100 volts and one second equal 100 centiseconds. By using these scale factors, the limiting initial conditions become:

Q_o = 3.08×10^5 $volts^3/cs$

V_{oi} = 2.5×10^3 volts/cs

r_i = 6.25 volts

r_o = 12.5 volts

r_{ci} = 25 volts

D_o = 0.394 volts

ρ_L = 7.95×10^{-9} lb-cs^2/volts^4

ρ_s = 23.4×10^{-9} lb-cs^2/volts^4

$\bar{\mu}_o$ = 2.91×10^{-8} lb-cs/volts^2 @ 80°F

In Eq. (4-19) let

$$B' = \left[\frac{\rho_s - \rho_L}{\rho_s + \frac{\rho_L}{2}}\right] \left[\frac{V_{oi}}{r_{ci}^n}\right]^2 \tag{5-1}$$

and

$$C' = \left[\frac{24\mu_o}{D_o^2}\right] \left[\frac{1}{\rho_s + \frac{\rho_L}{2}}\right] \tag{5-2}$$

By introducing two new parameters

$$B = \frac{V_i}{V_{oi}} \quad \frac{r_{ci}^n}{r_c}^2 \tag{5-3}$$

and

$$C = \left[\frac{D_o^2}{D^2} \quad \frac{\mu}{\bar{\mu}_o}\right] \tag{5-4}$$

which are dimensionless and include the two variables r_{ci} and D. These two variables are of major importance and are to be investigated as a function of time. They will be included in Eq. (4-19) as B'B and C'C. Substituting the constants in B' and C' gives

$$B' = \frac{1.76}{2} \times 10^8$$

$$C' = 165$$

Now let τ equal computer time in which

$$\tau = 100\, t \tag{5-5}$$

$$\frac{dr}{dt} = 100\, \frac{dr}{d\tau} \tag{5-6}$$

$$\frac{d^2r}{dt^2} = 10^4\, \frac{d^2r}{d}2 \tag{5-7}$$

Hence, Eq. (4-19) rewritten becomes

$$10^4\, \frac{d^2r}{d\tau^2} = \frac{1.76}{2} \times 10^8\, \frac{B}{r2} - 1.65 \times 10^4\, c\, \left(\frac{dr}{d\tau}\right)$$

or

$$\frac{d^2r}{d\tau^2} = \frac{1.76}{2} \times 10^4\, \frac{B}{r^2} - 1.65\, c\, \left(\frac{dr}{d\tau}\right) \tag{5-8}$$

For variation in particle size only the parameter C in Eq. (5-8) will change. By replacing C with y, then for a given particle size, y will vary only with $\frac{\mu}{\mu_o}$. For particle sizes ranging from 10μ to 100μ the following equations are applicable.

100μ

$$\ddot{r} = \frac{1.76}{2}\, \frac{10^4}{r^2}\, B - 1.65\, y\, \dot{r} \tag{5-9}$$

75μ

$$\ddot{r} = \frac{1.76}{2}\, \frac{10^4}{r^2}\, B - 2.92\, y\, \dot{r} \tag{5-10}$$

50μ

$$\ddot{r} = \frac{1.76}{2}\, \frac{10^4}{r^2}\, B - 6.6\, y\, \dot{r} \tag{5-11}$$

40μ

$$\ddot{r} = \frac{1.76}{2}\, \frac{10^4}{r^2}\, B - 10.3\, y\, \dot{r} \tag{5-12}$$

30μ

$$\ddot{r} = \frac{1.76}{2} \frac{10^4}{r^2} B - 18.35 y \dot{r} \qquad (5\text{-}13)$$

20μ

$$\ddot{r} = \frac{1.76}{2} \frac{10^4}{r^2} B - 41.3 y \dot{r} \qquad (5\text{-}14)$$

10μ

$$\ddot{r} = \frac{1.76}{2} \frac{10^4}{r^2} B - 165 y \dot{r} \qquad (5\text{-}15)$$

in which $y = \frac{\mu}{\bar{\mu}_o}$.

To program Eq. (5-9) through Eq. (5-15) on the Donner electrical analog the only difference will be an appropriate potentiometer setting providing for a variation in B and y. By letting B equal x and using an expression for y^2 developed by Kersten (12), x can be determined in terms of r_{ci} and y^2. The solution is as follows:

$$x = B = \left[\frac{V_i}{V_{oi}}\right] \frac{r_c}{r_{ci}} = (6.4 \times 10^{-7})\ v_i^2\ r_c \qquad (5\text{-}16)$$

$$\frac{\bar{\mu}}{\bar{\mu}_o} = 0.0016\ v_i\ r_c \qquad (5\text{-}17)$$

Solving for v_i from Eq. (5-17) gives

$$V_i^2 = \frac{(\frac{\bar{\mu}}{\bar{\mu}_o})^2\ 10^6}{(2.56)^2\ r_c} \qquad (5\text{-}18)$$

Hence

$$x = \frac{0.25}{r_c} \left(\frac{\mu}{\bar{\mu}_o}\right)^2 \qquad (5\text{-}19)$$

Table I presents the values of x and y which in turn are set on a potentiometer.

TABLE I

POTENTIOMETER SETTINGS

r_c	y	y^2	$\frac{0.25}{r_c}$	x
0.1	2.53	6.4	2.5	16.0
0.2	1.26	1.59	1.25	1.99
0.3	0.84	0.71	0.83	0.59
0.4	0.63	0.40	0.625	0.25
0.5	0.50	0.25	0.50	0.125
0.6	0.42	0.18	0.417	0.075
0.7	0.36	0.13	0.357	0.046
0.8	0.32	0.1025	0.313	0.032
0.9	0.25	0.0625	0.25	0.0156
1.2	0.21	0.044	0.208	0.0092
1.3	0.20	0.040	0.192	0.00768
1.4	0.18	0.032	0.179	0.00572
1.5	0.17	0.029	0.167	0.00485
2.0	0.13	0.0169	0.125	0.00211

Table II presents the values of r and cr^{-2} plotted in Fig. 6. These same r and cr^{-2} voltages are in turn set on the function generator by adjusting one set of break-voltage controls and the corresponding slope controls.

Figure 7 represents the circuit necessary for solving Eq. (5-9) through (5-15). The potentiometer values to be set for potentiometers P_{o4}, P_{o6}, and P_{o7} are constant. The potentiometer values to be set for potentiometers P_{o1}, and P_{o2} are found in Table I for a given value of r_c.

TABLE II

FUNCTION GENERATOR DATA

$r = \frac{17,600}{r^2}$ 1 inch = 100 volts

r (volts)	cr^{-2}(volts)
0.00	Indeterminate
15	78.00
20	43.90
25	27.15
30	19.55
40	11.00
50	7.04
60	4.89
70	3.59
80	2.75
90	2.17
100	1.76

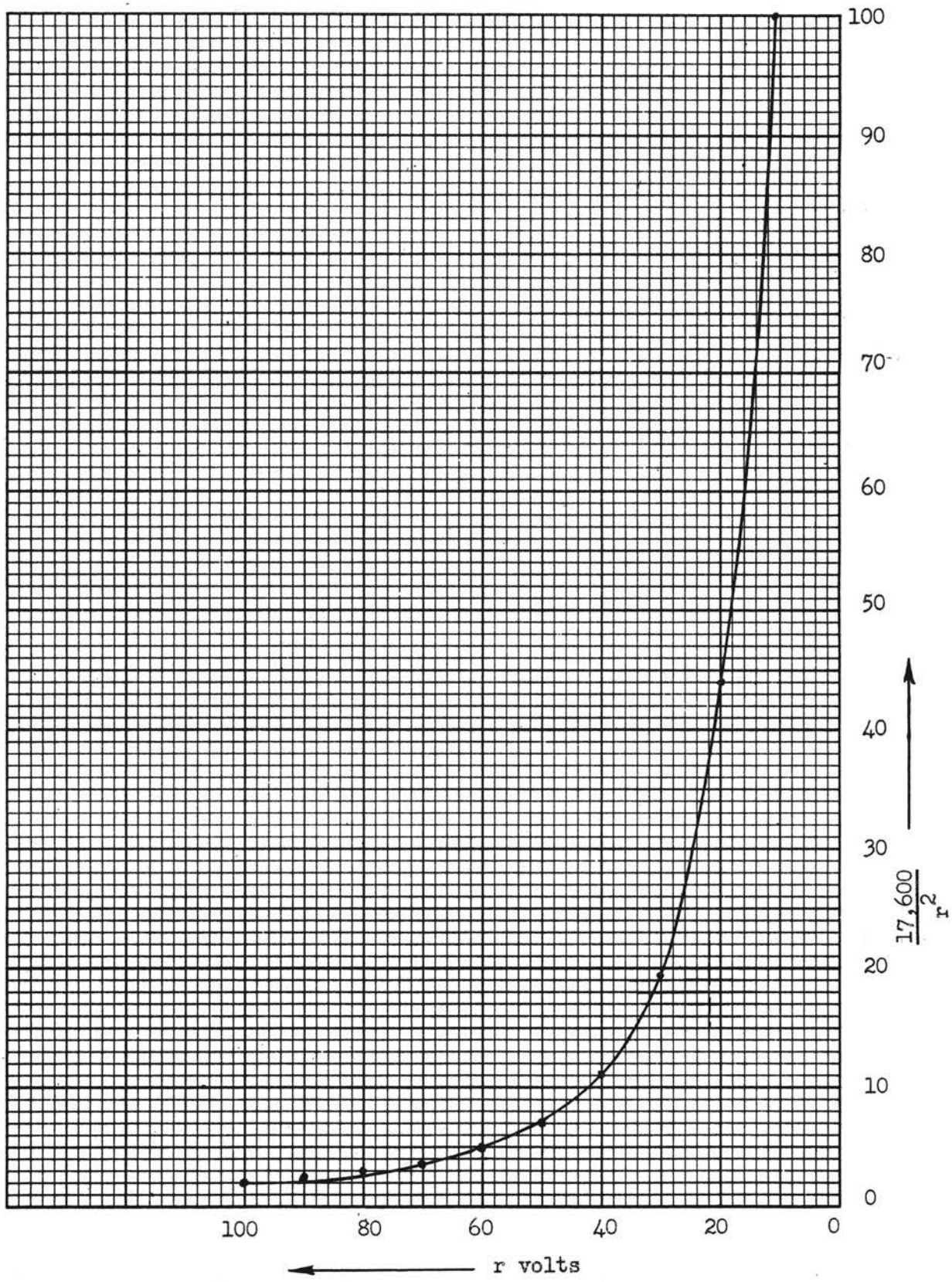

Figure 6. Function Generator Plot

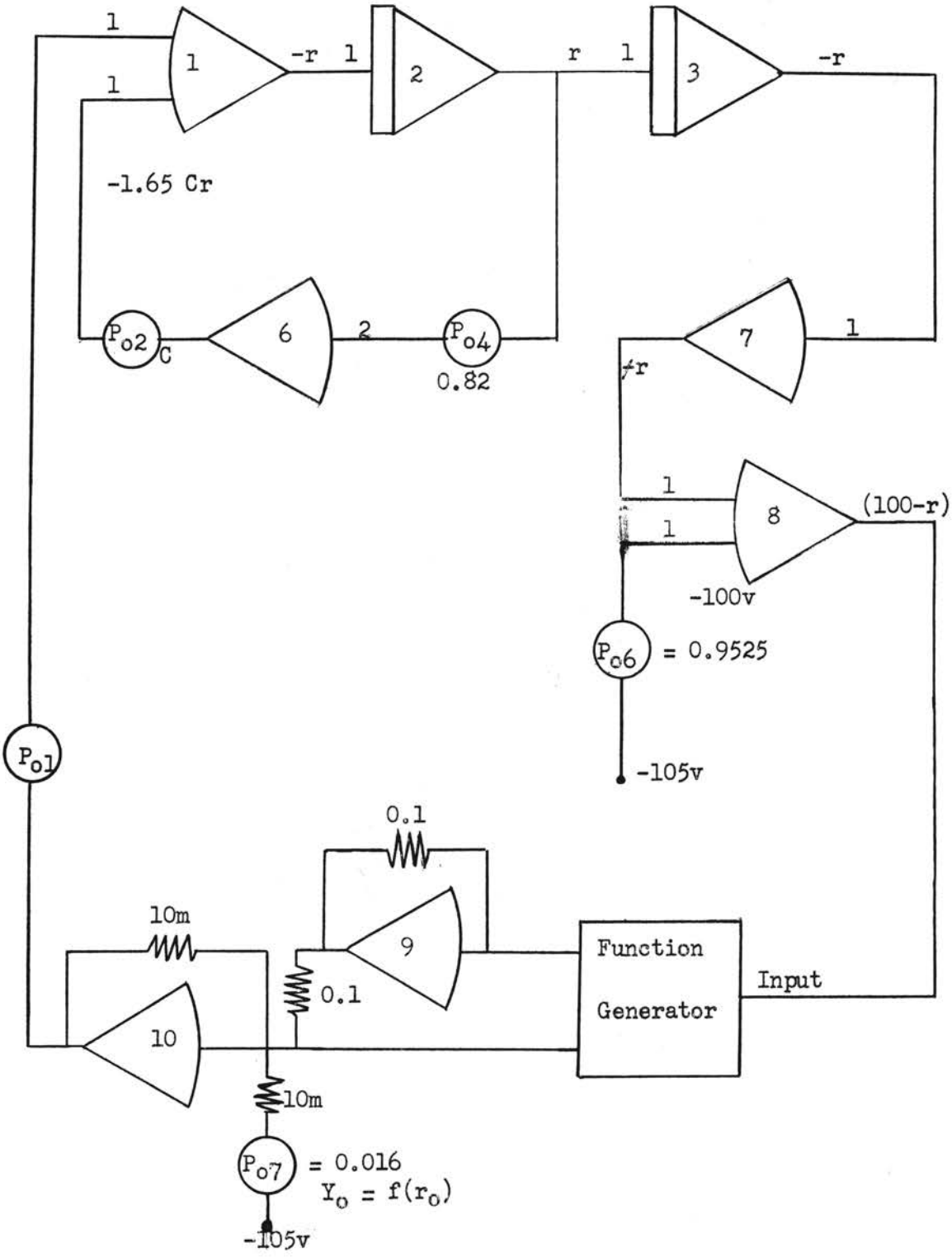

Figure 7. Problem Board Schematic

CHAPTER VI

RESULTS

This investigation presents the relative separation and the maximum size particle that a hydroclone may remove from a fluid. However, the results of the included data are valid only when the inlet, overflow, and underflow nozzle are equal to one-fourth of the hydroclone's diameter.

Plots of Eq. (4-19) solved on the Donner electrical analog are shown in Fig. 8. These curves represent different size particles plotted on a graph of distance versus time. However, the distance in this case is the distance that a particle of a given size would be from the hydroclone's axis in a given period of time. The period of time is one second and the flow rate is eight gallons per minute.

The size of the particles has a definite physical effect on the curves and can be easily noted in the figure. The larger size particle (D=100 microns) attained a greater radius than does the smaller size particle (D=10 microns) for any specified size hydroclone. As the particle size increased, the distance from the hydroclone's axis to the equilibrium radius also increased. Thus, as the particle size increased, the acceleration forces also increased which caused an overall increase in the solid elimination efficiency.

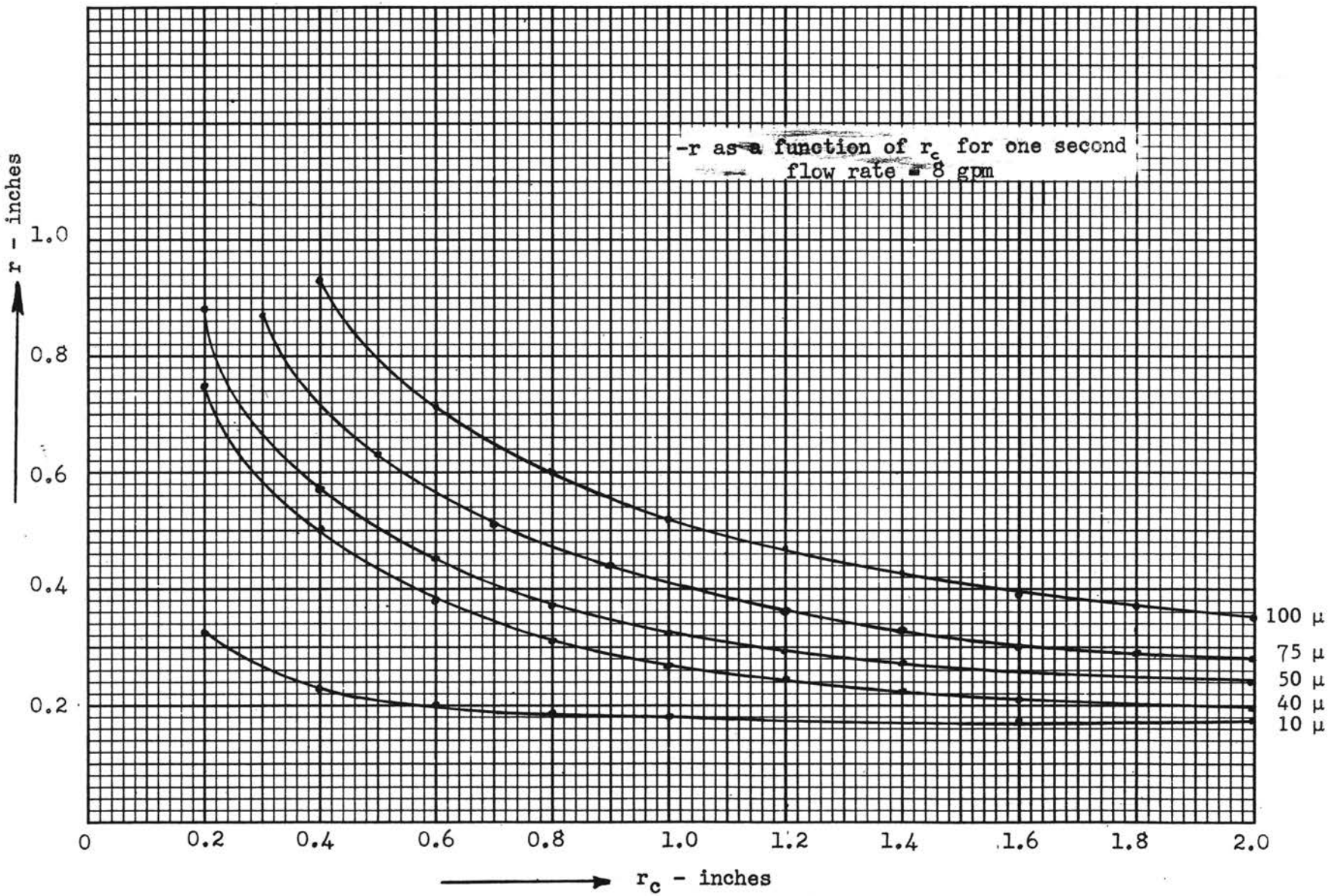

Figure 8. Separation Plot

To calculate pressure drop, Eq. (2-4) developed by Yosheoka and Hotta (1) was used. Yosheoka and Hotta also have experimentally proven this equation to be accurate within a plus or minus five percent. Table III represents the pressure drop through a hydroclone in feet of fluid flowing for different hydroclone diameters. By setting D_i, and D_{of} equal to $D_c/4$, and using the average value of K' (0.068), Eq. (2-4) was rewritten for a flow rate of eight gallons per minute as

$$\Delta P = \frac{745}{D_c^{4.1}}$$

TABLE III

HYDROCLONE DIAMETER VERSUS PRESSURE DROP

$$K' = 0.068 \quad \frac{(\text{ft. of liquid})(\text{in.})^{4.1}}{(\text{gal./min.})^{2.27}}$$

D_c (in.)	P (ft.)
2.00	43.4
1.75	75.25
1.50	141.00
1.25	298.00
1.00	745.00
0.75	2,400.00

CHAPTER VII

THEORETICAL DESIGN

The following hydroclone is theoretically designed to remove contaminating particles of 10 microns in size with a flow rate of eight gallons per minute. The other variables will be determined and fixed for these specific conditions.

From the condition that the vortex-finder radius must equal one-fourth of the hydroclone's radius, the size of the overflow nozzle is set, once the hydroclone radius is determined. From Fig. 8 where the particle displacement from the hydroclone's axis versus the hydroclone radius for different particle sizes, a hydroclone radius of 0.72 inches will give a 10 micron particle a displacement of 0.19 inches in one second and an overflow nozzle radius of 0.18 inches. Therefore, a 10 micron particle will not exit through the vortex-finder, but will be forced to the hydroclone's walls and exit through the underflow nozzle.

The inlet nozzle should be attached tangentially to the cylindrical section and at some small angle sufficient to give a small downward velocity component. This small angle β, determines the length of the vortex-finder into the top of the cylindrical section so that the incoming feed will not pass directly out

through the vortex-finder. Therefore, by assuming that the fluid after making one and a fourth revolutions, will be below the end of the vortex-finder, the length of the vortex-finder can be determined.

$$L_{vf} = 2.5\ D_c\ \text{TAN}\ \beta + D_i$$

Setting $\beta = 5$ degrees

$$L_{vf} = 3.6\ (0.087) + 0.36 = 0.673$$

Kelsall (6) states that the length of the cylindrical section should be one hydroclone diameter and that the included angle should be maintained between 10 and 15 degrees. Therefore, 12 degrees will be used in this design.

$$H_{cs} = 2(0.72) = 1.44 \text{ inches}$$

$$L_{tc} = \frac{(0.72)}{\text{TAN } 6^\circ} = \frac{(0.72)}{0.105} = 6.85 \text{ inches.}$$

Hence, for removing 10 micron size particles with a flow rate of eight gallons per minute, the following design is specified Fig. 9.

$D_{ci} = 1.44$ inches

$D_i = 0.36$ inches

$D_{of} = 0.36$ inches

$D_{uf} = 0.36$ inches

$L_{vf} = 0.673$ inches

$\theta = 12^\circ$

$\beta = 5^\circ$

$H_{cs} = 1.44$ inches

$L_t = 8.29$ inches

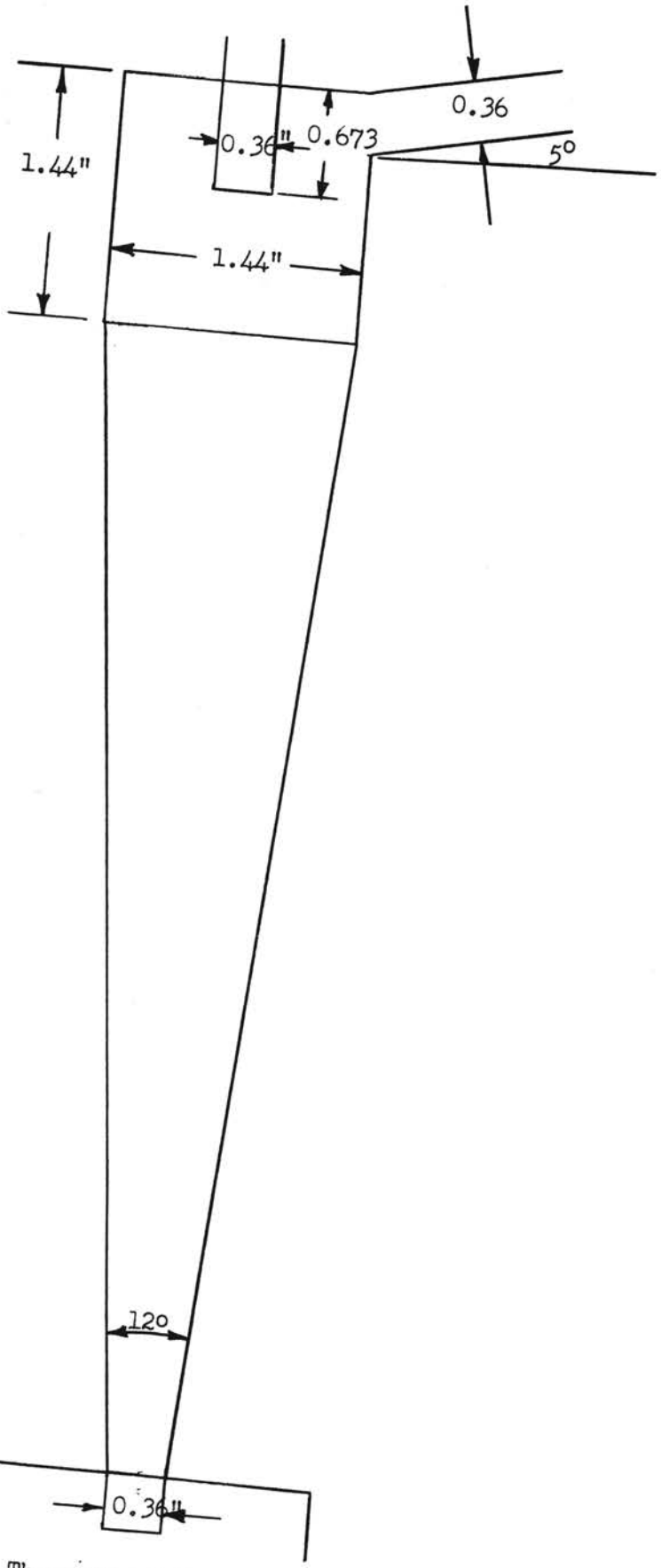

Figure 9. Theoretical Design Scale 1:1

From Eq. (6-1) the pressure drop through a hydroclone with a diameter of 1.44 inches would be 168 feet of fluid flowing. The fluid in this investigation was Mil-O-5606 hydraulic fluid with a mass density of 0.0309 lb. per cubic inch. Therefore, the pressure drop through the specified hydroclone is 62.3 psi.

In Fig. 9 the wall thickness is not drawn to scale because the working pressure will vary with each hydroclone.

CHAPTER VIII

SUMMARY AND CONCLUSIONS

The purpose of this investigation was to evaluate the functions of a hydroclone to eliminate contaminants from hydraulic fluids and to give an accurate assessment of the effects of the several hydroclone variables on liquid-solid separation. A constant flow rate of eight gallons per minute and that the overflow, underflow, and inlet nozzles equal one-fourth of the hydroclone's diameter were assumed in the derived expression.

In this analysis the following basic assumptions were made:

1. Criner (10) accurately described the flow pattern of the fluid within the hydroclone.

2. The air core within the vortex-finder may be eliminated.

3. Solids within the hydroclone assume the fluid velocity except where motion relative to the fluid is caused by centrifugal forces.

4. The radial acceleration must be considered in the design.

5. The forces of gravity and buoyancy may be neglected.

The differential equation developed governing the particle behavior upon entering a hydroclone in a viscous, incompressible medium is as follows:

$$\frac{d^2r}{dt^2} = \frac{\rho_s - \rho_L}{\rho_s + \frac{\rho_L}{2}} \left[\frac{V_{oi}}{r^n}\right]^2 r^{2n-1} - \left[\frac{24\ \mu_o\ V_R}{D_o^2\ \rho_s + \frac{\rho_L}{2}}\right] \qquad (4\text{-}19)$$

Equation (4-19) includes the effects of "eddying" in the turbulent viscosity term μ_o, and the forces necessary to accelerate the mass of fluid set in motion by a particle.

Navier-Stokes' equations for viscous flow were simplified and converted to cylindrical polar coordinates by the following limiting conditions:

1. The flow is steady.

2. The pressure difference within the system is small enough that the fluid medium may be considered to be incompressible.

3. The flow is two-dimensional.

Applying these conditions and replacing the partial derivatives with ordinary derivatives, Navier-Stokes' equation becomes:

$$\left[\frac{V_R}{r}\ \frac{d(Vr)}{dr}\right] = \frac{\mu}{\rho}\ \frac{d}{dr}\ \left[\frac{1}{r}\ \frac{d(Vr)}{dr}\right] \qquad (4\text{-}18)$$

Equation (4-18) was then solved for the radial velocity and substituted into Eq. (4-11), giving the final expression to be solved for a specific hydroclone. This expression took the form of Eq. (4-19), and was solved on the Donner electrical analog.

After scaling Eq. (4-19) to the Donner electrical analog, a plot of the distance that a given size particle would be from the hydroclone's axis as a function of the time was plotted versus the hydroclone's radius, Fig. 8. The time for this plot was set as one second.

The effects of different size particles in Fig. 8 can be easily noted. The fact that the larger-size-particle distance from the hydroclone's axis was greater than the distance for a small particle in a given time is due to the acceleration forces and the difference in mass of the two particles. Due to this difference in mass and the acceleration forces, the larger-size particles will have a larger equilibrium radius than the small-size particles.

The hydroclone's included angle according to Kelsall (6) should be maintained between 10 and 15 degrees. From this investigation the only effect that the included angle had on the solid elimination efficiency was to decrease the distance to the hydroclone's wall and to increase the overall length. As the length increased, the time for a given-size particle to be removed increased. However, if the angle is too small, mixing will occur in the truncated section. Therefore, 10 degrees should be set as the minimum angle for design purposes.

It can be concluded that Fig. 8 will accurately predict the size particle that a specified hydroclone will eliminate if the vortex-finder, overflow, and underflow nozzles are each set equal to one-fourth the hydroclone's diameter.

A SELECTED BIBLIOGRAPHY

1. Dahlstrom, D. A., Ph. D. Thesis, Northwestern University (1949).

2. Driessen, M. G., Review of Industrial Mining, St. Elienne, pp. 449-61 (March 31, 1951).

3. Criner, H. E., "The Vortex Thickener," International Conference on Coal Preparation, Paris (1950).

4. Nurmi, Whatley, and Engel, Chemical Engineering Progress, Vol. 50, No. 15, pp. 41 (1954).

5. Shepherd, C. B. and C. E. Lapple, "Flow Pattern and Pressure Drop in Cyclone Dust Collectors," Ind. and Eng. Chem. (1939) Vol. 31, pp. 972-984.

6. Kelsall, D. F., Presented to Inst. Mining Metallurgy, London, (September, 1952).

7. Banesji, S. K. and H. L. Roy, Trans. Indian Inst. Chem. Engrs., Vol. 6, No. 17.

8. Kelsall, D. F., Chemical Engineering Science, Vol. II, page 254 (1953).

9. Haas, P. A., E. O. Nurmi, M. E. Whatley, and T. R. Engel, Chemical Engineering Progress, Vol. 53, No. 4, pp. 203 (1957).

10. Criner, H. E., Paper presented at International Conference of Coal Preparation, Paris (1950).

11. Tietjens, Hydro and Aeromechanics, pp. 107 (1934).

12. Kersten, R. D., M. S. Thesis, Oklahoma State University (1957).

13. Moder, J. J., Ph. D. Thesis, Northwestern University (1950).

APPENDIX A

NOMENCLATURE

A_E	Area of overflow nozzle, sq. ft.
A_i	Area of feed nozzle, sq. ft.
b	Width of hydroclone entrance, in.
C_D	Drag coefficient of friction
D_o	Particle diameter, microns
D_c	Hydroclone diameter, in.
D_{ci}	Minimum hydroclone diameter, in.
D_i	Diameter of feed nozzle, in.
D_{of}	Diameter of overflow nozzle, in.
D_{uf}	Diameter of underflow nozzle, in.
F	Friction losses, ft.
F_a	Acceleration force, lb.
F_c	Centrifugal force, lb.
F_d	Drag force, lb.
F_{cv}	Friction loss of hydroclone/H_i, ft. per ft.
F_{ev}	Friction loss of exit/H_i, ft. per ft.
F_v	Friction loss of hydroclone and exit/H_i, ft. per ft.
F_o	Friction loss at entrance, ft.
ΔH	Pressure drop per unit length of fluid flowing, ft. per ft.
ΔH_v	Pressure drop/H_i, ft. per ft.

H_E	Velocity head at overflow nozzle, ft.
H_i	Velocity head at inlet nozzle, ft.
H_{cs}	Length of cylindrical section, in.
J	Coefficient of friction
K_1	Expansion factor to correct for entering feed
L_T	Total length of hydroclone, in.
L_{vf}	Length of vortex-finder, in.
P	Pressure, psi.
ΔP	Pressure drop, psi.
Q_o	Flow rate through hydroclone, gpm.
r	Variable radius of hydroclone, in.
r_{ci}	Minimum radius of hydroclone, in.
V_E	Velocity at overflow nozzle, ft. per sec.
V_i	Velocity at inlet nozzle, ft. per sec.
V_o	Average velocity at entrance, ft. per sec.
V_c	Velocity in outer spiral within hydroclone, in. per sec.
V_R	Radial velocity, in. per sec.
V_t	Tangential velocity, in. per sec.
V_{oi}	Initial inlet velocity, in. per sec.
t	Time, sec.

Greek Letters

π	Pi
Δ	Delta
μ	Mu, absolute viscosity, lb force per sq in.

ρ_L	Rho, mass density of liquid, lb mass per cu in.
ρ_s	Rho, mass density of solid, lb mass per cu in.
$\bar{\mu}_o$	Mu, initial turbulent viscosity, lb force per sq in.
$\bar{\mu}$	Mu, turbulent viscosity, lb force per sq in.
τ	Tau, computer time, sec.
ν	Nu, kinematic viscosity, centistokes
ω	Omega, angular speed, radians per sec.
$\emptyset$	Phi, cylindrical polar coordinate in plane where A is constant
β	Beta, included feed angle, degrees

Abbreviations

lb	Pounds
cu	Cubic
psi	Pounds per square inch
sq	Square
ft	Feet
sec	Seconds
in.	Inch, inches
gpm	Gallons per minute

Symbols

%	Percent
∇	An operator

VITA

James Fred Beattie

Candidate for the Degree of

Master of Science

Thesis: AN OPTIMUM DESIGN FOR A HYDROCLONE USING ELECTRICAL ANALOG TECHNIQUES

Major Field: Mechanical Engineering

Biographical:

Personal Data: Born near Midland, Michigan, May 12, 1937, the son of Richard H. and Eva P. Beattie.

Education: Attended grade school in Kelly and Greendale, Michigan and Weleetka, Oklahoma. Graduated from Weleetka High School in 1955. Received the Bachelor of Science degree from Oklahoma State University with a major in Mechanical Engineering in August, 1959. Completed requirements for the Master of Science degree in August, 1961.

Professional Experience: Graduate assistant for two years at Oklahoma State University. Instructor at University of Oklahoma since January 16, 1961.

Member of Sigma Tau, A. S. M. E., A. S. C. E. and A. I. M. E.